Association of Cognitive Impairment With Free Water in the Nucleus Basalis of Meynert and Locus Coeruleus to Transentorhinal Cortex Tract

Winston Thomas Chu, PhD, Wei-en Wang, PhD, Laszlo Zaborszky, MD, PhD, Todd Eliot Golde, MD, PhD, Steven DeKosky, MD, Ranjan Duara, MD, David A. Loewenstein, PhD, Malek Adjouadi, PhD, Stephen A. Coombes, PhD, and David E. Vaillancourt, PhD

Correspondence

Dr. Vaillancourt vcourt@ufl.edu

Neurology® 2022;98:e700-e710. doi:10.1212/WNL.000000000013206

Abstract

Background and Objectives

The goal of this work was to determine the relationship between diffusion microstructure and early changes in Alzheimer disease (AD) severity as assessed by clinical diagnosis, cognitive performance, dementia severity, and plasma concentrations of neurofilament light chain.

Methods

Diffusion MRI scans were collected on cognitively normal participants (CN) and patients with early mild cognitive impairment (EMCI), late mild cognitive impairment, and AD. Free water (FW) and FW-corrected fractional anisotropy were calculated in the locus coeruleus to transentorhinal cortex tract, 4 magnocellular regions of the basal forebrain (e.g., nucleus basalis of Meynert), entorhinal cortex, and hippocampus. All patients underwent a battery of cognitive assessments; neurofilament light chain levels were measured in plasma samples.

Results

FW was significantly higher in patients with EMCI compared to CN in the locus coeruleus to transentorhinal cortex tract, nucleus basalis of Meynert, and hippocampus (mean Cohen d = 0.54; $p_{\rm fdr} < 0.05$). FW was significantly higher in those with AD compared to CN in all the examined regions (mean Cohen d = 1.41; $p_{\rm fdr} < 0.01$). In addition, FW in the hippocampus, entorhinal cortex, nucleus basalis of Meynert, and locus coeruleus to transentorhinal cortex tract positively correlated with all 5 cognitive impairment metrics and neurofilament light chain levels (mean $r^2 = 0.10$; $p_{\rm fdr} < 0.05$).

Discussion

These results show that higher FW is associated with greater clinical diagnosis severity, cognitive impairment, and neurofilament light chain. They also suggest that FW elevation occurs in the locus coeruleus to transentorhinal cortex tract, nucleus basalis of Meynert, and hippocampus in the transition from CN to EMCI, while other basal forebrain regions and the entorhinal cortex are not affected until a later stage of AD. FW is a clinically relevant and noninvasive early marker of structural changes related to cognitive impairment.

From the J. Crayton Pruitt Family Department of Biomedical Engineering (W.T.C., D.E.V.), Department of Applied Physiology and Kinesiology (W.T.C., W.-e.W., S.A.C., D.E.V.), Department of Neuroscience (T.E.G.); Center for Translational Research in Neurodegenerative Diseases (T.E.G.), Department of Neurology (S.D., D.E.V.), and McKnight Brain Institute (S.D., D.E.V.), University of Florida, Gainesville; Center for Molecular and Behavioral Neuroscience (L.Z.), Rutgers University, Newark, NJ; Wein Center for Alzheimer's Disease and Memory Disorders (R.D., D.A.L.), Mount Sinai Medical Center, Miami Beach; Center for Cognitive Neuroscience and Aging (D.A.L.) and Department of Psychiatry and Behavioral Sciences (D.A.L.), University of Miami Miller School of Medicine; and Center for Advanced Technology and Education (M.A.), Florida International University, Miami.

Go to Neurology.org/N for full disclosures. Funding information and disclosures deemed relevant by the authors, if any, are provided at the end of the article.

Glossary

AD = Alzheimer disease; ADRC = Alzheimer's Disease Research Center; ANCOVA = analysis of covariance; CDR-SB = Clinical Dementia Rating–Sum of Boxes; CN = cognitively normal; dMRI = diffusion MRI; DTI = diffusion tensor imaging; EMCI = early MCI; FA_t = FW-corrected fractional anisotropy; frPSI = Failure to Recover from Proactive Semantic Inference; FSL = FMRIB Software Library; FW = free water; LASSI-L = Loewenstein-Acevedo Scale for Semantic Interference and Learning; LMCI = late MCI; MCI = mild cognitive impairment; MMSE = Mini-Mental State Examination; MNI = Montreal Neurological Institute; MoCA = Montreal Cognitive Assessment; ROI = region of interest; SUVR = standardized uptake value ratio.

Extracellular β -amyloid aggregates and intracellular tau lesions are pathologic hallmarks of AD. However, other markers of neurodegeneration are strong predictors of AD clinical symptoms. Free water (FW) is a diffusion MRI (dMRI) measure that estimates the volume fraction of extracellular space and is increased under conditions of neurodegeneration. Recent findings suggest that, compared to atrophy, FW may be a more effective early marker of neurodegeneration. However, it is unclear how FW relates to clinical diagnosis, clinical measures, and assays of global neurodegeneration such as plasma neurofilament light chain.

Human postmortem studies suggest that Alzheimer disease (AD)-associated tau pathology progresses from the locus coeruleus to nucleus basalis of Meynert to transentorhinal cortex to entorhinal cortex to hippocampus to neocortex. We calculated FW in regions and tracts relevant to early AD and related it to patient diagnosis, cognitive performance, dementia severity, and neurofilament light chain. We hypothesized that FW would be elevated in the locus coeruleus to transentorhinal cortex tract and nucleus basalis of Meynert in the lower dementia severity groups and that other regions will be affected only as dementia severity progressed. We further predicted that FW would correlate with clinical measures and plasma neurofilament light chain concentration.

Methods

Participants

Data were collected as a part of the 1Florida Alzheimer's Disease Research Center (ADRC). A comprehensive list of procedures and diagnostic criteria for the 1Florida ADRC study has been given previously. 10 The full inclusion and exclusion criteria are given in eAppendix 1, links.lww.com/ WNL/B702. Data used in the current study were derived from 152 participants who were cognitively normal (CN) or had diagnoses of early mild cognitive impairment (EMCI), late mild cognitive impairment (LMCI), and AD. These cognitive diagnoses, which are independent of the etiologic diagnoses, were determined with the 1Florida ADRC diagnostic algorithm.11 The full criteria for the cognitive diagnoses are included in eAppendix 2. Notably, EMCI differs from LMCI in performance on Clinical Dementia Rating-Sum of Boxes (CDR-SB; EMCI 0.5-2.0, LMCI 2.5-4.0) and Hopkins Verbal Learning Test-Revised delayed recall or

Wechsler Memory Scale 4th Edition delayed paragraph recall scores (EMCI 1–1.5 SD, LMCI 1.5–2 SD below age, education, and ethnic/cultural norms).

Table 1 provides the demographics and clinical characteristics of each group. Clinical assessments in this study included the CDR-SB, 12 Montreal Cognitive Assessment (MoCA), 13 Mini-Mental State Examination (MMSE), 14 and Loewenstein-Acevedo Scale for Semantic Interference and Learning (LASSI-L). 15 The LASSI-L assessment focused on the cued recall B2 intrusions sensitive to the ability to recover from proactive semantic inference (LASSI-L frPSI) and participants' delayed recall (LASSI-L delay) scores, given that these scores have been shown to best discriminate between CN and pre–mild cognitive impairment (MCI) compared to the other LASSI-L indices. 15,16 Furthermore, the LASSI-L frPSI has been shown to correlate with hippocampal and entorhinal cortex volume and amyloid load. 15,16 Only clinical assessment data collected within 6 months of the imaging date were included in the study

Standard Protocol Approvals, Registrations, and Patient Consents

All participants gave written informed consent, and all procedures were approved by the local Institutional Review Board. The work described has been carried out in accordance with the Code of Ethics of the World Medical Association (Declaration of Helsinki) for experiments involving humans.

Data Availability

Anonymized data are available from the corresponding author on reasonable request.

dMRI Acquisition

dMRI scans were acquired on a 3T Siemens Magnetom Skyra (Erlangen, Germany) with a 20-channel head/neck coil. The diffusion scans were acquired with a whole-brain echo planar sequence and the following parameters: diffusion directions 64, b value 1,000 s/mm², number of b0 images 1, repetition time 9,000 milliseconds, echo time 90 milliseconds, flip angle 90°, in-plane resolution 2×2 mm, slice thickness 2 mm (no gap), acquisition matrix 125×125 in plane, and number of slices 64.

dMRI Data Analysis

dMRIs were processed with image processing tools from the FMRIB Software Library (FSL¹⁷), Advance Normalization

Table 1 Patient Characteristics

	CN	EMCI	LMCI	AD	Statistic (p value)
No.	30	77	23	22	
Age, y	70.5 ± 6.7	72.8 ± 7.9	75.3 ± 7.8	71.5 ± 9.2	F = 1.78 (0.15)
M/F, n	9/21	35/42	14/9	12/10	$\chi^2 = 5.79 (0.12)$
Education, y	16.3 ± 2.9	15.9 ± 3.2	15.5 ± 3.0	15.1 ± 3.9	F = 0.59 (0.63)
CDR-SB score	0.0 ± 0.1	1.0 ± 0.5	3.2 ± 0.5	7.6 ± 4.1	F = 119.27 (1.31E-38)
MMSE score	29.3 ± 1.0	28.2 ± 1.9	25.5 ± 3.7	19.1 ± 7.8	F = 43.83 (7.33E-20)
MoCA score	25.4 ± 2.1	22.3 ± 3.8	20.1 ± 4.9	14.4 ± 6.5	F = 21.10 (1.72E-10)
LASSI-L frPSI score	11.5 ± 1.9	8.5 ± 2.8	7.7 ± 3.5	4.3 ± 2.8	F = 18.07 (4.87E-09)
LASSI-L delayed recall score	20.5 ± 3.3	13.6 ± 6.4	7.4 ± 7.9	6.8 ± 6.9	F = 16.23 (2.17E-08)
APOE ε4 carriers (0/1+), n	22/7	46/23	13/9	10/12	$\chi^2 = 5.50 (0.14)$
Neurofilament light chain, pg/mL	13.3 ± 4.7	18.4 ± 10.0	23.7 ± 13.5	34.4 ± 30.5	F = 8.01 (6.4E-05)
Amyloid status (-/+), n	19/3	36/17	12/10	0/18	χ^2 = 34.43 (1.98E-07)
Global amyloid SUVR	1.05 ± 0.13	1.18 ± 0.23	1.24 ± 0.28	1.46 ± 0.18	F = 10.31 (3.78E-06)

Abbreviations: AD = Alzheimer disease; CDR-SB = Clinical Dementia Rating-Sum of Boxes; CN = cognitively normal; EMCI = early mild cognitive impairment; frPSI = Failure to Recover From Proactive Semantic Inference; LASSI-L = Loewenstein-Acevedo Scale for Semantic Interference and Learning; LMCI = late mild cognitive impairment; MMSE = Mini-Mental State Examination; MoCA = Montreal Cognitive Assessment; SUVR = standardized uptake value ratio. Mean (± SD) values are given for demographic, clinical measures, and biomarkers levels stratified by group. The right-most column gives the group-effect test statistics and p value.

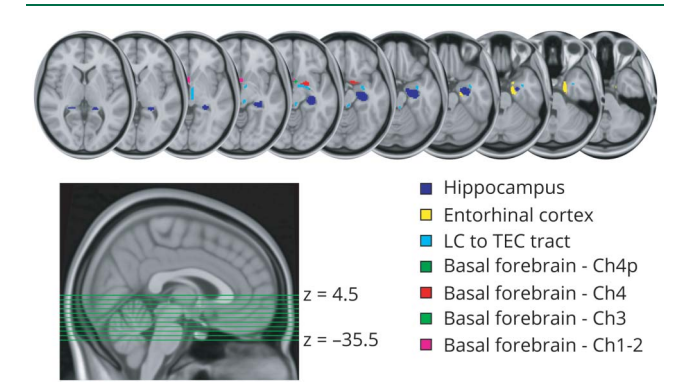
Tools, 18 and custom UNIX shell scripts. The dMRI processing pipeline was completely automated, and the results were consistent with previous work. 5 Scans were corrected for distortions due to eddy currents and head motion with affine transformations. The gradient directions were subsequently rotated to reflect these corrections, 19 and nonbrain tissue regions were removed from the scans. FW is a metric that can be calculated from a dMRI scan to estimate the fractional volume of freely diffusing water in each voxel. FW maps were calculated from the diffusion scans with a custom MATLAB script³ (MathWorks, Natick, MA), and the implementation of this technique is consistent with previous work.^{5,6,20} The distribution of FW in each of the 7 regions of interest (ROIs) is given in histogram plots in eFigure 1, links.lww.com/WNL/ B702. In addition to the FW map, a set of adjusted diffusion tensors was created in which the partial volume effects of FW were eliminated. Fractional anisotropy was calculated from the FW-corrected diffusion tensors using FSL's DTIFit²¹ to create FW-corrected fractional anisotropy (FA_t) maps.

Subject-space diffusion tensor imaging (DTI) and FW maps were registered to the Montreal Neurological Institute (MNI) 152 template space 22 for application of standard ROIs to conform to the MNI152 template space. The registration technique used in this study was chosen on the basis of a previously published literature review comparing registration techniques. 5,20 Registration to standard space was performed by nonlinearly warping FA $_{\rm t}$ and FW maps using Advanced Normalization Tools in R to FA $_{\rm t}$ and FW templates, respectively.

Seven ROIs were examined in this study: locus coeruleus to transentorhinal cortex tract, 4 magnocellular regions of the basal forebrain, entorhinal cortex, and hippocampus (Figure 1). Here, the term region refers to a continuous area. These ROIs were chosen on the basis of previous literature indicating that they are affected in the early stages of AD. Hippocampal ROIs were acquired from the Harvard-Oxford subcortical atlas through FSL.²³ Entorhinal cortex ROIs were acquired from the Human Brainnetome Atlas.²⁴ Four basal forebrain ROIs containing the magnocellular cell groups were acquired from a previous study that mapped histologic sections to MNI space²⁵ that included the septum (Ch1-2), the horizontal limb of the diagonal band (Ch3), the sublenticular nucleus (Ch4; nucleus basalis of Meynert), and the posterior portion of the sublenticular nucleus (Ch4p). Tracts connecting the locus coeruleus and transentorhinal cortex were acquired from the Brainstem Connectome Atlas²⁶ on the basis of connectome imaging data from the Human Connectome Project.²⁷ For each region, the average FW and FA_t values across the entire region were calculated. All regions showed significant correlations (mean $r^2 = 0.53$; $p_{fdr} < 0.001$) between left and right values for both FW and FA_t metrics. Thus, left and right regions were combined in the final analysis to reduce the dimensionality of the classifiers and to simplify interpretation of the results.

To develop a more detailed understanding of the change in FW along the locus coeruleus to transentorhinal cortex tract, a slice-wise analysis was performed. Average FW values were

Figure 1 Regions of Interest



Examined regions of interest are shown in transverse plane slices overlaid on top of the Montreal Neurological Institute (MNI) 152 template. Locations of the transverse plane slices shown are designated on the sagittal plane image. The z-direction coordinates designate the superior-most and inferior-most slice in MNI space. Total field of view of the diffusion scan covered the entire brain. LC = locus coeruleus; TEC = transentorhinal cortex.

calculated within 2-dimensional slices along the locus coeruleus to transentorhinal cortex tracts. The locus coeruleus to transentorhinal cortex tract curves and changes direction; thus, it was important for the slice direction to change accordingly. Tracts were sliced in the y-direction in the portion of the tract connecting the locus coeruleus to the thalamus region (y = -37 to -7). Tracts were then sliced in the x-direction as the tract extended laterally toward the temporal lobes (left tract: x = -10 to -28, right tract: x = 10 to 29). The final portion of the tract ran inferiorly to terminate in the transentorhinal cortex; this portion was sliced in the z-direction (z = -15 to -33).

APOE Genotyping

Blood samples were genotyped for the APOE $\epsilon 2$, $\epsilon 3$, and $\epsilon 4$ alleles with predesigned TaqMan SNP Genotyping Assays for single nucleotide proteins rs7412 and rs429358 (Thermo Fisher Scientific, Waltham, MA) on the QuantStudio 7 Flex Real-Time PCR system (Applied Biosystems, Foster City, CA) following the manufacturer's protocol. A positive APOE carrier status was defined as the presence of ≥ 1 $\epsilon 4$ alleles because this has been associated with an increased risk of developing AD.²⁸

Amyloid PET Imaging

Amyloid PET scans were performed with the [¹⁸F] florbetaben tracer. The methodology for PET scanning and rating has been previously described.^{9,29,30} Global amyloid status (+/-) was determined by an independent, trained radiologist and a trained, experienced rater (R.D.). Both raters were blinded to the cognitive and clinical diagnosis, and a high interrater concordance has been reported.^{30,31} Global amyloid standardized uptake value ratios (SUVRs) were calculated for comparison with the use of previously described methods.^{9,29,30}

Plasma Neurofilament Light Chain

Immediately after blood draw, blood samples were centrifuged to obtain plasma. Samples were stored at -80° C and

subsequently shipped to the Quanterix Corp (Lexington, MA). Samples were analyzed with the Simoa NF-light kit on the Quanterix Simoa HD-1 Analyzer. All samples were tested in duplicates within the assay dynamic range.

Statistical Methods

For the between-group analyses, analyses of covariance (ANCOVAs) were performed with the group (CN, EMCI, LMCI, AD) as the primary factor while adjusting for the effects of sex, age, years of education, and *APOE* ϵ 4 carrier status. For regions in which significant group effects were detected, post hoc t tests were performed compared to controls (CN vs EMCI, CN vs LMCI, and CN vs AD) and for LMCI vs AD. Partial correlation analyses between imaging metrics and clinical measures were performed with the Spearman nonparametric rank-order correlation adjusted for the effects of age, sex, years of education, *APOE* ϵ 4 carrier status, and group. All reported p values were corrected for false discovery rate, p32 and the significance threshold was set to p6dr < 0.05.

Results

Demographics, Clinical Assessment, and Biomarker Data

Demographic, clinical assessment, amyloid status, global amyloid SUVR, APOE carrier status, and neurofilament light chain data stratified by different groups are depicted in Table 1. One hundred fifty-two participants were included in this study and had diagnoses of CN (n = 30), EMCI (n = 77), LMCI (n = 23), or AD (n = 22). No significant differences in age, sex, or years of education were found between different clinical diagnosis groups. Participants had a mean age of 72.1 \pm 8.0 years, a female ratio of 54%, and an average of 15.9 \pm 3.4 years of education attained. As expected, significant between-group differences were found in CDR-SB, MMSE, MoCA, and LASSI-L scores (mean $F = 43.7 p_{fdr} < 1.0E-07$). Post hoc t tests confirmed that CDR-SB score is higher (AD > LMCI > EMCI > CN; mean Cohen d = 2.62; $p_{\text{fdr}} < 1.0\text{E-}05$) and MMSE score is higher (AD < LMCI < EMCI < CN; mean Cohen d = -0.97; $p_{\text{fdr}} < 0.005$) with greater diagnostic severity. Post hoc t tests on MoCA scores revealed a significant reduction in score between CN and EMCI (EMCI < CN; Cohen d = -0.93; $p_{\text{fdr}} < 5.0\text{E}-05$) and between LMCI and AD (AD < LMCI; Cohen d = -1.04; $p_{\text{fdr}} <$ 0.05) but not between EMCI and LMCI. Post hoc t tests on LASSI-L frPSI scores revealed significant reductions in scores between CN and EMCI (EMCI < CN; Cohen d = -1.18; p_{fdr} < 1.0E-05) and between LMCI and AD (AD < LMCI; Cohen d =-1.16; $p_{\rm fdr} < 0.05$) but not between EMCI and LMCI. While the post hoc t tests on LASSI-L delayed recall scores revealed a significant reduction in score between CN and EMCI (EMCI < CN; Cohen d = -1.24; $p_{\text{fdr}} < 5.0\text{E}-07$), differences were not found between EMCI and LMCI or between LMCI and AD.

Significant between-group differences were found in amyloid status ($\chi^2 = 34.43$), global amyloid SUVR (F = 10.31), and

Table 2 Group-wise Comparisons

		Group effect	Group effect	CN-EMCI	CN-LMCI	CN-AD	LMCI-AD
Region	Metric	F statistic	p Value				
Hippocampus	FW	19.04	4.93E-09 ^c	1.02E-03 ^c	1.47E-04 ^c	5.71E-06 ^c	2.97E-02 ^a
Basal forebrain (Ch4)	FW	13.65	7.01E-07 ^c	2.27E-02 ^a	1.79E-02 ^a	5.59E-06 ^c	9.73E-03 ^b
Locus coeruleus to transentorhinal cortex tract	FW	10.43	1.31E-05 ^c	4.86E-02 ^a	1.54E-02 ^a	1.07E-03 ^c	4.51E-02 ^a
Entorhinal cortex	FW	10.72	1.25E-05 ^c	1.83E-01	2.07E-01	3.79E-04 ^c	3.22E-03 ^c
Basal forebrain (Ch4p)	FW	9.46	3.24E-05 ^c	5.87E-01	5.59E-01	1.40E-04 ^c	1.38E-03 ^c
Basal forebrain (Ch1-2)	FW	7.05	4.84E-04 ^c	6.74E-02	7.76E-02	1.71E-04 ^c	6.74E-02
Basal forebrain (Ch3)	FW	4.32	1.25E-02 ^a	1.09E-01	4.14E-01	1.02E-02 ^a	1.09E-01
Basal forebrain (Ch1-2)	FA_t	3.77	2.20E-02 ^a	5.49E-03 ^b	3.70E-02 ^a	5.28E-03 ^b	1.08E-01
Basal forebrain (Ch4)	FA _t	2.57	8.33E-02				
Entorhinal cortex	FA_{t}	2.54	8.33E-02				
Basal forebrain (Ch3)	FA_{t}	2.23	1.12E-01				
Basal forebrain (Ch4p)	FA _t	2.06	1.27E-01				
Hippocampus	FA _t	1.07	3.91E-01				
Locus coeruleus to transentorhinal cortex tract	FA _t	0.86	4.62E-01				

Abbreviations: AD = Alzheimer disease; CN = cognitively normal; EMCI = early mild cognitive impairment; LMCI = late mild cognitive impairment; FA_t = FW-corrected fractional anisotropy; FW = free water.

Regions with significant between-group effects and post hoc test results: The effects of sex, age, education, and APOE ϵ 4 carrier status were included in the analyses of variance as covariates. Post hoc t tests were performed between controls and disease groups for regions in which there was a significant group effect. The p values are corrected for the false discovery rate (${}^{a}p_{fdr} < 0.05$, ${}^{b}p_{fdr} < 0.01$, ${}^{c}p_{fdr} < 0.005$).

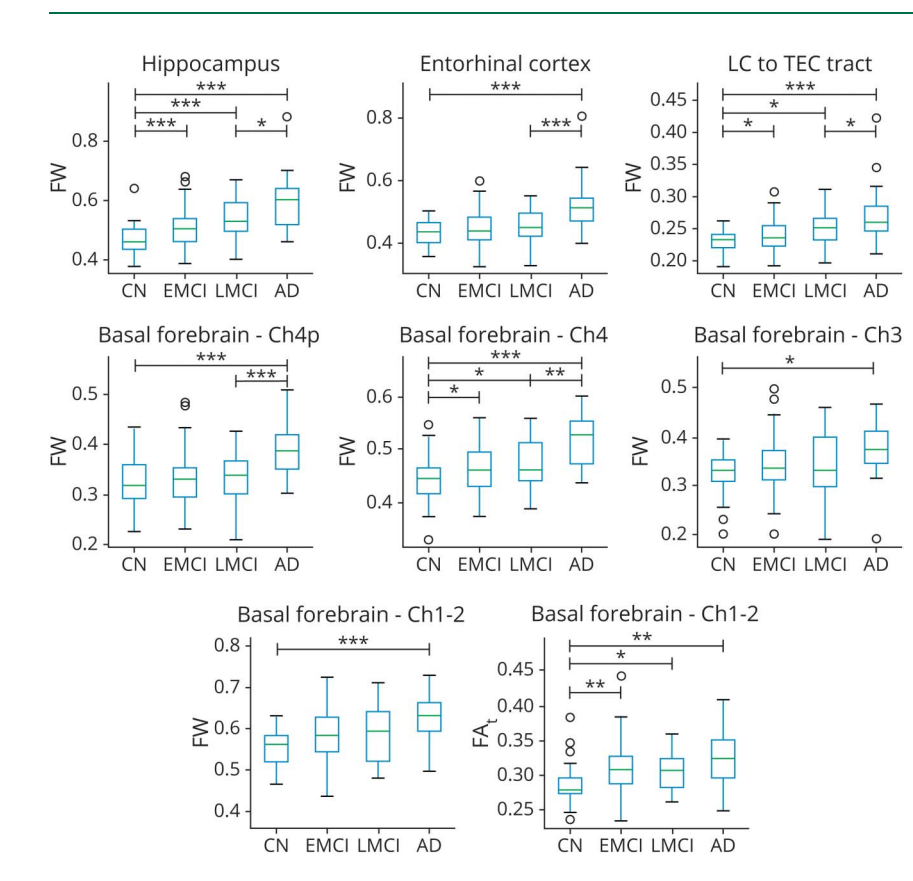
neurofilament light chain (F=8.01) ($p_{\rm fdr}<1.0$ E-04) but not in *APOE* &4 carrier status. Post hoc t tests revealed a significant difference in amyloid status between LMCI and AD (AD > LMCI; $\varphi=0.93$; $p_{\rm fdr}<0.005$) but not between EMCI and LMCI or between CN and EMCI. Global amyloid SUVR was significantly different between CN and EMCI (EMCI > CN; Cohen d=0.62; $p_{\rm fdr}<0.01$) and between LMCI and AD (AD > LMCI; Cohen d=0.94; $p_{\rm fdr}<0.01$) but not between EMCI and LMCI. Neurofilament light chain was significantly different between CN and EMCI (EMCI > CN; Cohen d=0.58; $p_{\rm fdr}<0.01$) but not between EMCI and LMCI or between LMCI and AD.

FW Is Higher With Worsened Clinical Diagnosis Severity

Results examining the effect of the clinical diagnosis group on FW are given in Table 2 and displayed graphically in Figure 2. ANCOVAs calculating the effect of group on FW while covarying for the effects of sex, age, education, and APOE &4 carrier status revealed significant group effects in the hippocampus, entorhinal cortex, locus coeruleus to transentorhinal cortex tract, Ch4p, Ch4, Ch3, and Ch1-2 (mean F=10.68; $p_{\rm fdr}<0.05$). Post hoc t tests showed broadly that higher FW was associated with greater disease severity. FW was significantly higher in EMCI compared to CN in the locus coeruleus to transentorhinal cortex tract, nucleus basalis of Meynert, and hippocampus (mean Cohen d=0.54; $p_{\rm fdr}<0.05$). FW

was significantly higher in AD compared to CN in all 7 examined regions (mean Cohen d=1.41; $p_{\rm fdr}<0.01$). A significant effect of group was found on FA_t in Ch1-2 (F=3.77; $p_{\rm fdr}<0.05$). Post hoc t tests revealed that higher FA_t in Ch1-2 was associated with greater disease severity. Regions and dMRI metrics in which significant group effects were found are shown in Figure 2. An identical analysis was performed in which amyloid status was added as a covariate to the ANCOVAs. The results from this analysis are given in eTable 1, links.lww.com/WNL/B702. A significant effect of group on FW was found in all 7 regions (hippocampus, entorhinal cortex, locus coeruleus to transentorhinal cortex tract, Ch4p, Ch4, Ch3, and Ch1-2) (mean F=5.33; $p_{\rm fdr}<0.05$). A significant effect of group on FA_t was found in Ch1-2 and Ch4 (mean F=3.10; $p_{\rm fdr}<0.05$).

A slice-wise analysis of the locus coeruleus to transentorhinal cortex tract was performed to determine in which sections of the tract there were significant differences in FW between the groups. Figure 3 shows the fluctuations in FW along the left and right locus coeruleus to transentorhinal cortex tract and the slices in which there were significant group effects. For example, the first section of the right locus coeruleus to transentorhinal cortex tract (sliced in the y-direction) extends from the locus coeruleus to the thalamus and resides predominantly in the brainstem. Only the 3 most anterior slices of this section contained significant group effects (mean F =



Significant group-wise comparisons ($p_{\rm fdr}$ < 0.05) of free water (FW) and FW-corrected fractional anisotropy (FA_t). Post hoc t tests were performed (cognitively normal [CN] vs early mild cognitive impairment [EMCI], CN vs late mild cognitive impairment [LMCI], CN vs Alzheimer disease [AD], and LMCI vs AD) and were corrected for the false discovery rate (* $p_{\rm fdr}$ < 0.05, ** $p_{\rm fdr}$ < 0.01, *** $p_{\rm fdr}$ < 0.005). Small circles designate outliers (±1.5 times the interquartile range). Ch4 = Basal nucleus of Meynert; LC = locus coeruleus; TEC = transentorhinal cortex.

5.53; $p_{\rm fdr}$ < 0.05). The second section (sliced in the x-direction) extends laterally and passes through the basal forebrain region. All slices in this section manifested a significant group effect (mean F = 7.59; $p_{\text{fdr}} < 0.05$). Post hoc tests revealed that 10, 4, and 2 of the 10 slices had higher FW in AD compared to CN (mean Cohen d = 1.21; $p_{\text{fdr}} < 0.01$), LMCI compared to CN (mean Cohen d = 0.82; $p_{\text{fdr}} < 0.05$), and EMCI compared to CN (mean Cohen d = 0.60; $p_{\text{fdr}} <$ 0.05) respectively. The 2 slices in which FW was higher in EMCI compared to CN are located in the anterior medial portion of the tract that passes through the nucleus basalis of Meynert.²⁵ The third section (sliced in the z-direction) extends inferiorly and terminates in the transentorhinal cortex. Eight of the 10 slices in this section contained a significant group effect (mean F = 6.14; $p_{fdr} < 0.05$). Post hoc tests in this anterolateral portion of the tract revealed significantly higher FW only in patients with AD compared to CN (mean Cohen $d = 1.00; p_{\rm fdr} < 0.005).$

Correlations Among FW, Clinical Measures, and Neurofilament Light Chain

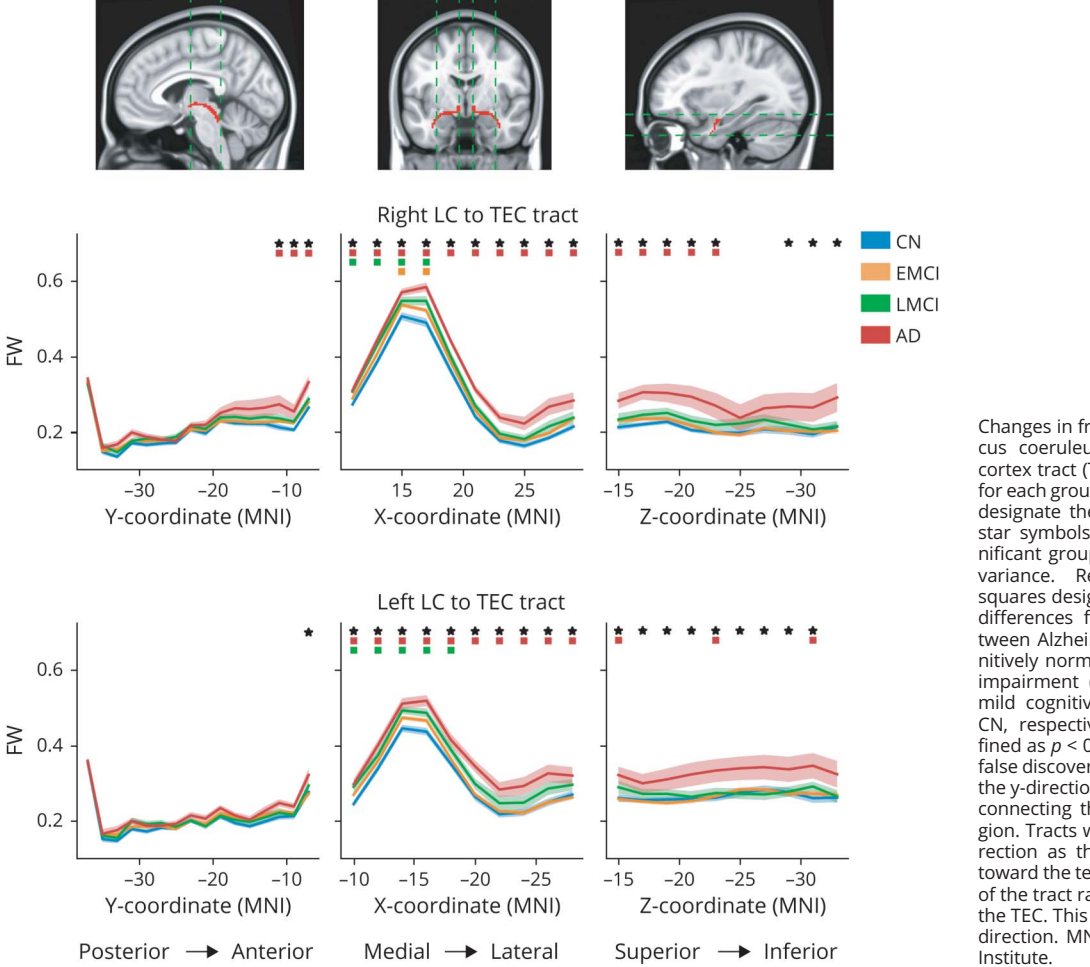
Spearman rank correlation coefficients were calculated across imaging measures, clinical measures, and neurofilament light chain while controlling for the effects of age, sex, education, *APOE* £4 carrier status, and group (Figure 4). FW in the hippocampus, entorhinal cortex, locus coeruleus to transentorhinal cortex tract, and Ch4 correlated significantly with

MoCA, CDR-SB, MMSE, and both LASSI-L scores (mean r^2 = 0.10; $p_{\rm fdr}$ < 0.05). FW in the other basal forebrain regions correlated intermittently with clinical measures. FA_t in the examined regions correlated sparsely with the clinical measures. Significant correlations were found between plasma neurofilament light chain and FW in the hippocampus, entorhinal cortex, locus coeruleus to transentorhinal cortex tract, Ch4, and Ch3 (mean r^2 = 0.06; $p_{\rm fdr}$ < 0.05). No significant correlations were found between plasma neurofilament light chain and FA_t.

Discussion

In this study, we found that FW was significantly higher in patients with AD compared to CN individuals in the hippocampus, 4 basal forebrain regions (Ch4, Ch4p, Ch3, Ch1-2), locus coeruleus to transentorhinal cortex tract, and entorhinal cortex. FW was significantly higher in patients with LMCI compared to CN individuals and in those with EMCI compared to CN individuals in 3 regions: the hippocampus, Ch4, and locus coeruleus to transentorhinal cortex tract. Within the locus coeruleus to transentorhinal cortex tract, group effects were evident in FW in the anterior portions of the tract spanning the region of the basal forebrain and the transentorhinal cortex. Correlation analyses revealed that higher FW was associated with lower performance on cognitive

Figure 3 FW in the Locus Coeruleus to Transentorhinal Cortex Tract



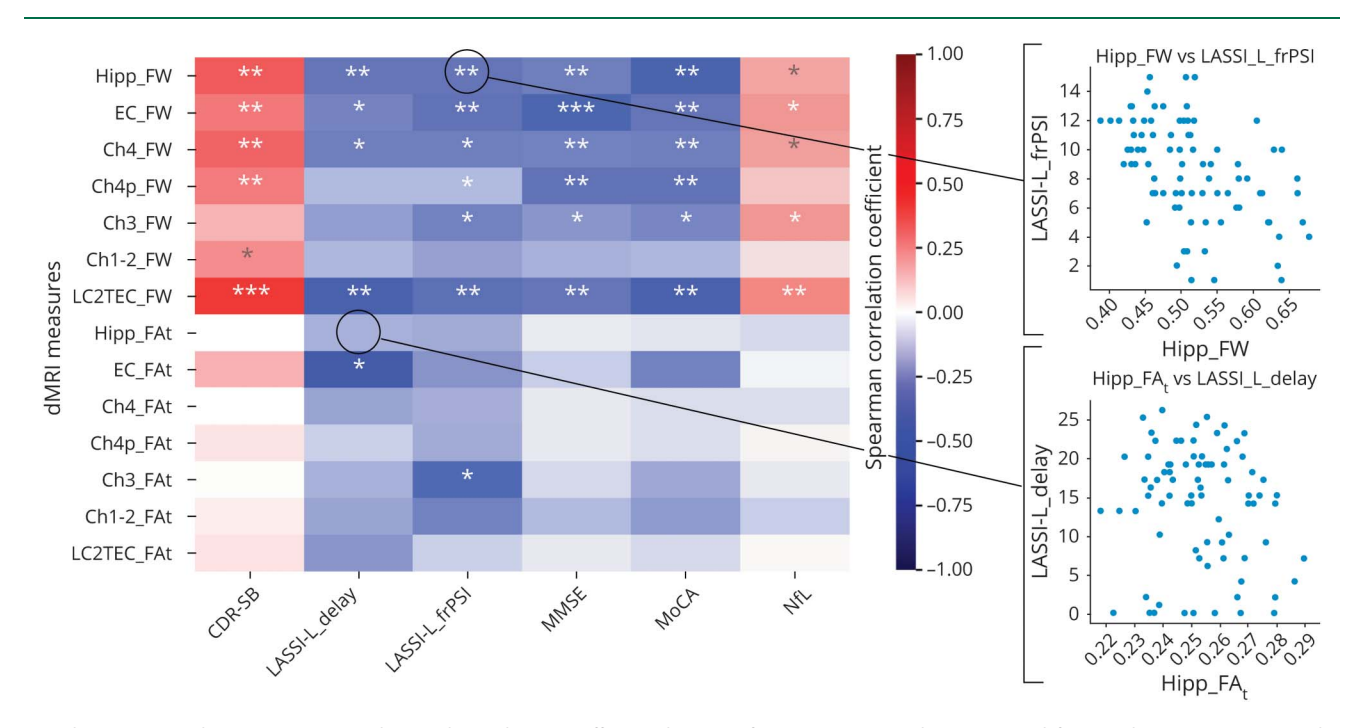
Changes in free water (FW) along the locus coeruleus (LC) to transentorhinal cortex tract (TEC) are plotted separately for each group. Semitransparent regions designate the SEM at each slice. Black star symbols designate slices with significant group effects in the analysis of variance. Red, green, and orange squares designate slices with significant differences from post hoc t tests between Alzheimer disease (AD) and cognitively normal (CN), late mild cognitive impairment (LMCI) and CN, and early mild cognitive impairment (EMCI) and CN, respectively. Significance was defined as p < 0.05 after correction for the false discovery rate. Tracts were sliced in the y-direction in the portion of the tract connecting the LC to the thalamus region. Tracts were then sliced in the x-direction as the tract extended laterally toward the temporal lobes. Final portion of the tract ran inferiorly to terminate in the TEC. This portion was sliced in the zdirection. MNI = Montreal Neurological

measures (MoCA, MMSE, and LASSI-L) and with greater dementia severity (CDR-SB). FW in 5 of the 7 examined regions was also significantly correlated with neurofilament light chain. Together, these results provide evidence in support of a progressive disease model in which neurodegeneration occurs early in the anterior medial portion of the locus coeruleus to transentorhinal cortex tract, nucleus basalis of Meynert (Ch4), and hippocampus. In a later stage, the anterior lateral portion of the locus coeruleus to transentorhinal cortex tract, entorhinal cortex, and other basal forebrain regions manifest significant neurodegeneration and AD symptom progression.

The progression of pathology and neurodegeneration that precedes clinically manifested AD is not clearly understood. One of the earliest staging models of AD progression asserted that tau pathology first occurs in the entorhinal cortex. It has subsequently been proposed on the basis of larger-scale pathology studies that pathologic tau first occurs in the locus coeruleus before spreading to the transentorhinal cortex and then neocortex through neuron-to-neuron propagation. In

this study, we found that patients with EMCI, LMCI, and AD had significantly higher FW compared to CN individuals when averaging across the entire locus coeruleus to transentorhinal cortex tract. Our results show that AD-related neurodegeneration occurs within the locus coeruleus to transentorhinal cortex tract and is detectable in patients with EMCI compared to CN individuals. Our finding that the anterior medial portion of the tract passing through the nucleus basalis of Meynert is affected in patients with EMCI while the portion of the tract approaching the transentorhinal cortex is affected only in AD is consistent with a nucleus basalis of Meynert to entorhinal cortex AD progression model.³⁴ Group effects were not observed in the brainstem portion of the tract extending superiorly and anteriorly from the locus coeruleus to the region of the thalamus. Although studies have reported tau pathology in the locus coeruleus and locus coeruleus atrophy in the earliest stages of AD, 8,35 it should be noted that the brainstem is notoriously difficult to image reliably, given its small size and high physiologic noise relative to the rest of the brain. 36-38 It is also possible that the CN group may contain participants with locus coeruleus or

Figure 4 FW Correlates With Clinical Measures and Neurofilament Light Chain



Correlation matrix shows Spearman rank partial correlation coefficients between free water (FW) and FW-corrected fractional anisotropy (FA_t) in the examined regions, clinical measures, and neurofilament light chain while controlling for the effects of age, sex, education, *APOE* ε 4 carrier status, and group. Color of each square designates the value of the correlation coefficient: dark red designates a strong positive correlation; dark blue designates a strong negative correlation; and white designates no correlation. Asterisks designate the *p* value after false discovery rate correction: * r_{tdr} < 0.05, * r_{tdr} < 0.01, ** r_{tdr} < 0.005. Examined regions: hippocampus (Hipp), entorhinal cortex (EC), magnocellular regions of the basal forebrain (Ch4, Ch4p, Ch3, and Ch1-2), and locus coeruleus to transentorhinal cortex tract (LC2TEC). CDR-SB = Clinical Dementia Rating–Sum of Boxes; dMRI = diffusion MRI; frPSI = Failure to Recover from Proactive Semantic Inference; LASSI-L = Loewenstein-Acevedo Scale for Semantic Interference and Learning; MMSE = Mini-Mental State Examination; MoCA = Montreal Cognitive Assessment; NfI = neurofilament light chain.

entorhinal cortex degeneration but without detectable cognitive deficits.

Although it is known that the basal forebrain plays an important role in AD progression, it is unknown how basal forebrain degeneration relates to and is sequenced in degeneration in other regions affected in AD such as the neocortex, hippocampus, and entorhinal cortex. In this study, we show that FW is progressively higher in the nucleus basalis of Meynert of patients with EMCI, LMCI, and AD compared to CN individuals, while no significant differences were found in the other basal forebrain cholinergic regions and the entorhinal cortex between patients with EMCI and CN individuals or between those with LMCI and CN individuals. These results align with a nucleus basalis of Meynert → entorhinal cortex → neocortex model of disease progression^{34,39} and suggest that neurodegeneration parallels the anatomic progression of tau pathology. These results also align with those that have reported preferential atrophy in the nucleus basalis of Meynert compared to the other subregions of the basal forebrain cholinergic system. 40,41

The effect of group on FA_t was significant only in the Ch1-2 region and was higher in patients with EMCI, LMCI, and AD compared to CN individuals. While dMRI has classically been

applied to white matter tracts, numerous studies have used dMRI to examine gray matter areas. 42-45 The measure FA quantifies the degree of direction-dependent diffusion. In white matter, FA values tend to be higher while in gray matter FA values are lower. Prior studies suggest that in an acute injury model, increased anisotropy (FA) is linked to the coherent organization of reactive astrocytes and gliosis. 42 The administration of 1-methyl-4-phenyl-1,2,3,6-tetrahydropyridine in a murine model of Parkinson disease demonstrated that FA measures derived from DTI decreased 5 to 7 days after injection and were thought to be related to the number of substantia nigra dopaminergic neurons. 44 The authors suggested that DTI can provide an indirect measure of dopaminergic neurodegeneration within the substantia nigra because cell loss in the substantia nigra alters the microstructural integrity and diffusivity of water molecules.⁴⁴ In the regions studied here such as the hippocampus, entorhinal cortex, and basal forebrain, they include complex tissue structures that could be reflected in diffusion measurements, including FA. In a mouse model of basal forebrain cholinergic degeneration, it was found that FA increased in the basal forebrain with reduced choline acetyl transferase-positive neurons. 45 The authors of this study proposed that a loss of isotropic (cholinergic) gray matter cells led to a greater contribution from residual anisotropic cells/ axons to the diffusion signals. 45 The contrasting effects of axon

degeneration (leading to decreases in FA) and cholinergic neuron degeneration (leading to increases in FA) complicate the interpretation of our FA_t results and suggest that patients with EMCI, LMCI, and AD compared to CN individuals had higher FA_t in Ch1-2 because this region experienced cholinergic neuron degeneration without axon degeneration. It is possible that higher FA_t in the other examined regions was not observed because both axon degeneration and cholinergic degeneration occurred. FA_t in regions such as the hippocampus, entorhinal cortex, and basal forebrain is likely further confounded by the occurrence of multiple fiber orientations within the same voxel.

Prior work has shown that the entorhinal cortex undergoes atrophy in patients with AD, 46,47 entorhinal cortex volume in patients with MCI predicts conversion to AD, ⁴⁸ and atrophy of the entorhinal cortex is predicted by atrophy of the basal forebrain. 34,39 Our finding that FW in the entorhinal cortex is higher in patients with AD compared to CN aligns with these findings that atrophy occurs in the entorhinal cortex of patients with AD. No significant differences in FW were found between patients with MCI (early and late) and CN individuals in the entorhinal cortex. Furthermore, FW in the portion of the locus coeruleus to transentorhinal cortex tract that approached the transentorhinal cortex was not significantly different between patients with MCI and CN individuals, although FW was higher in patients with AD compared to CN individuals. Our results suggest that, compared to the hippocampus and nucleus basalis of Meynert, FW in the entorhinal cortex is less affected in patients with MCI. However, it is possible that we did not observe differences between MCI and CN in the entorhinal cortex because the CN group may have already undergone some neurodegenerative changes. Thus, longitudinal analyses with time points well before MCI onset will be needed to definitively show the anatomic progression trends observed in this study.

The hippocampus plays a critical role in memory and is well known to atrophy in AD. 6,49 The hippocampus was included in this study as a reference point for the other examined regions. Our results replicate previous findings that FW in the hippocampus is higher in patients with EMCI, LMCI, and AD compared to CN individuals. 6

Our results that FW correlated positively with cognitive impairment and dementia severity as measured by the MoCA, MMSE, and CDR-SB supports previous studies that have found that atrophy of the hippocampus, entorhinal cortex, and basal forebrain positively correlates with cognitive impairment. The LASSI-L is a novel cognitive stress test that uniquely examines the ability to recover from proactive semantic interference in addition to delayed recall. The LASSI-L frPSI and LASSI-L delay have shown promise in discriminating between CN individuals and patients with pre-MCI and correlate with hippocampal atrophy, entorhinal cortex atrophy, and amyloid load. Si, Our finding of significant correlations (mean $r^2 = 0.01$; $p_{\rm fdr} < 0.05$) between LASSI-L performance (delayed recall and frPSI) and FW in the

hippocampus, locus coeruleus to transentorhinal cortex tract, entorhinal cortex, and nucleus basalis of Meynert provides supporting evidence that LASSI-L performance is an early marker of neurodegeneration related to cognitive impairment. Together, these results align with our hypothesis that FW is a noninvasive marker of neurodegeneration and show that the differences in FW that we observed are associated with measurable differences in cognitive impairment.

Finally, neurofilament light chain is a cytoplasmic protein highly expressed in myelinated axons such that increases in CSF and blood plasma have been associated with axonal damage. ⁵² Plasma neurofilament light chain is increased in patients with MCI and AD compared to CN individuals. ⁵³ In this study, we found that FW correlates positively with plasma neurofilament light chain. These data align with our hypothesis and provide important evidence that the observed higher FW represents neurodegeneration, although it is also possible that other mechanisms related to neuroinflammation could play an additional role.

One limitation of this study is the heterogeneity of patients with MCI. In this study, diagnoses were based on cognitive assessments, and it is possible that some of the patients with MCI may not eventually progress to AD. In a longitudinal study of 87 patients with MCI, it was found that at a 3-year follow-up visit, 77% of patients with amyloid-positive MCI developed AD, whereas 19% of patients with amyloid-negative MCI developed AD. Thus, some of the participants with MCI could be in the early stages of other types of dementia such as dementia with Lewy bodies or vascular dementia.

In this study, we examined FW in 152 patients ranging in cognitive abilities from CN to EMCI to LMCI to AD. Quantifying FW in 7 regions relevant to early AD pathology, we showed that higher FW is associated with greater clinical diagnosis severity, lower cognitive and functional performance, and higher plasma neurofilament light chain. The hippocampus, nucleus basalis of Meynert, and locus coeruleus to transentorhinal cortex tract had significantly higher FW in patients with EMCI compared to CN individuals, suggesting that these regions may begin to degenerate at an earlier stage of AD progression compared to the other cholinergic basal forebrain nuclei and the entorhinal cortex. It is important to note that not all patients with MCI convert to AD and that future longitudinal studies examining FW in these regions may identify those patients with MCI who are most likely to progress to AD. Overall, our results show that FW imaging is a noninvasive and clinically relevant imaging marker that is sensitive to early changes in cognitive impairment. However, replication in other datasets and further refinement are needed before FW imaging is used as an AD clinical trial endpoint for disease-modifying therapeutics.

Study Funding

Funding provided by NIH T32-NS082128, NIH P30-AG066506, NIH P50-AG047266, NIH P30 AG066506,

NIH R01-NS052318, NIH, 2RF1-NS023945-28, and NSF CNS-192018.

Disclosure

The authors report no disclosures relevant to the manuscript. Go to Neurology.org/N for full disclosures.

Publication History

Appendix Authors

Wei-en Wang,

Received by *Neurology* April 22, 2021. Accepted in final form November 30, 2021.

• • •		
Name	Location	Contribution
Winston T. Chu, PhD	University of Florida, Gainesville	Designed and conceptualized study; acquired the data; analyzed the data; interpreted the data; performed statistical analysis; drafted the manuscript for intellectual content

University of Florida,

Gainesville

Laszlo Zaborszky, MD, PhD	Rutgers University, Newark, NJ	Developed the postmortem mask of the Ch compartments; interpreted the data; revised the manuscript for intellectual content
Todd E. Golde, MD, PhD	University of Florida, Gainesville	Designed and conceptualized study
Steven T. DeKosky, MD	University of Florida, Gainesville	Interpreted the data; revised the manuscript for intellectual content

Acquired the data; interpreted the

data; revised the manuscript for

intellectual content

Rajan Duara, MD	Mount Sinai Medical Center, Miami Beach, FL	Interpreted the data; revised the manuscript for intellectual content
David A. Loewenstein, PhD	University of Miami, FL	Interpreted the data; performed statistical analysis; revised the manuscript for intellectual content

Malek Adjouadi, PhD	Florida International University, Miami	Interpreted the data; performed statistical analysis; revised the manuscript for intellectual content
Stephen A. Coombes, PhD	University of Florida, Gainesville	Designed and conceptualized study; interpreted the data; revised the manuscript for intellectual content
David F	University of Florida	Designed and severeturalized

Vaillancourt, Gainesville study; PhD perfor revise	ned and conceptualized interpreted the data; med statistical analysis; d the manuscript for ctual content
--	---

References

- Braak H, Braak E. Diagnostic criteria for neuropathologic assessment of Alzheimer's disease. Neurobiol Aging. 1997;18(4):S85-S88.
- Savva GM, Wharton SB, Ince PG, Forster G, Matthews FE, Brayne C. Age, neuropathology, and dementia. N Engl J Med. 2009;360(22):2302-2309.
- Pasternak O, Sochen N, Gur Y, Intrator N, Assaf Y. Free water elimination and mapping from diffusion MRI. Magn Reson Med. 2009;62(3):717-730.
- Ofori E, Pasternak O, Planetta PJ, et al. Longitudinal changes in free-water within the substantia nigra of Parkinson's disease. *Brain*. 2015;138(8):2322-2331.
- Archer DB, Bricker JT, Chu WT, et al. Development and validation of the Automated Imaging Differentiation in Parkinsonism (AID-P): a multicentre machine learning study. Lancet Digit Health. 2019;1(5):e222-e231.
- Ofori E, DeKosky ST, Febo M, et al. Free-water imaging of the hippocampus is a sensitive marker of Alzheimer's disease. NeuroImage Clin. 2019;24:101985.

- Braak H, Braak E. Neuropathological stageing of Alzheimer-related changes. Acta Neuropathol. 1991;82(4):239-259.
- Braak H, Thal DR, Ghebremedhin E, Del Tredici K. Stages of the pathologic process in Alzheimer disease: age categories from 1 to 100 years. J Neuropathol Exp Neurol. 2011;70(11):960-969.
- 9. 1Florida ADRC. Accessed November 15, 2020. 1floridaadrc.org.
- Barker W, Quinonez C, Greig MT, et al. Utility of plasma neurofilament light in the 1Florida Alzheimer's Disease Research Center (ADRC). J Alzheimers Dis. 2020;13:
- Duara R, Loewenstein DA, Greig M, et al. Reliability and validity of an algorithm for the diagnosis of normal cognition, mild cognitive impairment, and dementia: implications for multicenter research studies. Am J Geriatr Psychiatry. 2010;18(4):363-370.
- Hughes CP, Berg L, Danziger WL, Coben LA, Martin RL. A new clinical scale for the staging of dementia. Br J Psychiatry. 1982;140(6):566-572.
- Nasreddine ZS, Phillips NA, Bédirian V, et al. The Montreal Cognitive Assessment, MoCA: a brief screening tool for mild cognitive impairment. J Am Geriatr Soc. 2005; 53(4):695-699.
- Folstein MF, Folstein SE, McHugh PR. "Mini-Mental State": a practical method for grading the cognitive state of patients for the clinician. J Psychiatr Res. 1975;12(3): 189-198.
- Loewenstein DA, Curiel RE, Greig MT, et al. A novel cognitive stress test for the detection of preclinical Alzheimer disease: discriminative properties and relation to amyloid load. Am J Geriatr Psychiatry. 2016;24(10):804-813.
- Crocco EA, Loewenstein DA, Curiel RE, et al. A novel cognitive assessment paradigm to detect pre-mild cognitive impairment (PreMCI) and the relationship to biological markers of Alzheimer's disease. J Psychiatr Res. 2018;96:33-38.
- Leemans A, Jones DK. The B-matrix must be rotated when correcting for subject motion in DTI data. Magn Reson Med. 2009;61(6):1336-1349.
- FSL. Accessed November 15, 2020. fsl.fmrib.ox.ac.uk/fsl/fslwiki/.
- 19. Advanced Normalization Tools. Accessed November 15, 2020. stnava.github.io/ANTs/.
- Mitchell T, Archer DB, Chu WT, et al. Neurite orientation dispersion and density imaging (NODDI) and free-water imaging in Parkinsonism. Hum Brain Mapp. 2019; 40(17):5094-5107.
- Basser PJ, Mattiello J, LeBihan D. MR diffusion tensor spectroscopy and imaging. Biophys J. 1994;66(1):259-267.
- Mazziotta J, Toga A, Evans A, et al. A probabilistic atlas and reference system for the human brain: International Consortium for Brain Mapping (ICBM). *Philos Trans R* Soc Lond B Biol Sci. 2001;356(1412):1293-1322.
- Frazier JA, Chiu S, Breeze JL, et al. Structural brain magnetic resonance imaging of limbic and thalamic volumes in pediatric bipolar disorder. Am J Psychiatry. 2005; 162(7):1256-1265.
- Fan L, Li H, Zhuo J, et al. The human Brainnetome atlas: a new brain atlas based on connectional architecture. Cereb Cortex. 2016;26(8):3508-3526.
- Zaborszky L, Hoemke L, Mohlberg H, Schleicher A, Amunts K, Zilles K. Stereotaxic probabilistic maps of the magnocellular cell groups in human basal forebrain. NeuroImage. 2008;42(3):1127-1141.
- NeuroImaging Tools & Resources Collaboratory. Brainstem Connectome Atlas. Accessed November 15, 2020. nitrc.org/projects/brainstem_atlas/.
- Sun W, Tang Y, Qiao Y, et al. A probabilistic atlas of locus coeruleus pathways to transentorhinal cortex for connectome imaging in Alzheimer's disease. NeuroImage. 2020;223:117301.
- Farrer LA, Cupples LA, Haines JL, et al. Effects of age, sex, and ethnicity on the association between apolipoprotein E genotype and Alzheimer disease: a metaanalysis. APOE and Alzheimer Disease Meta Analysis Consortium. JAMA. 1997; 278(16):1349-1356.
- Sabri O, Seibyl J, Rowe C, Barthel H. Beta-amyloid imaging with florbetaben. Clin Transl Imaging. 2015;3(1):13-26.
- Duara R, Loewenstein DA, Lizarraga G, et al. Effect of age, ethnicity, sex, cognitive status and APOE genotype on amyloid load and the threshold for amyloid positivity. Neuroimage Clin. 2019;22:101800.
- Loewenstein DA, Curiel RE, DeKosky S, et al. Utilizing semantic intrusions to identify amyloid positivity in mild cognitive impairment. Neurology. 2018;91(10):e976-e984.
- Benjamini Y, Hochberg Y. Controlling the false discovery rate: a practical and powerful approach to multiple testing. J R Stat Soc Ser B (Methodological). 1995;57(1): 289-300.
- Braak H, Del Tredici K. Alzheimer's pathogenesis: is there neuron-to-neuron propagation? Acta Neuropathol. 2011;121(5):589-595.
- Fernández-Cabello S, Kronbichler M, Van Dijk KRA, et al. Basal forebrain volume reliably predicts the cortical spread of Alzheimer's degeneration. *Brain*. 2020;143(3): 993-1009.
- Grudzien A, Shaw P, Weintraub S, Bigio E, Mash DC, Mesulam MM. Locus coeruleus neurofibrillary degeneration in aging, mild cognitive impairment and early Alzheimer's disease. Neurobiol Aging. 2007;28(3):327-335.
- Nagae-Poetscher LM, Jiang H, Wakana S, Golay X, van Zijl PCM, Mori S. Highresolution diffusion tensor imaging of the brain stem at 3 T. AJNR Am J Neuroradiol. 2004;25(8):1325-1330.
- Brooks JC, Faull OK, Pattinson KT, Jenkinson M. Physiological noise in brainstem fMRI. Front Hum Neurosci 2013;7:623.
- Chu WT, Mitchell T, Foote KD, Coombes SA, Vaillancourt DE. Functional imaging
 of the brainstem during visually-guided motor control reveals visuomotor regions in
 the pons and midbrain. *Neuroimage*. 2021;226:117627.
- Schmitz TW, Nathan Spreng R. Basal forebrain degeneration precedes and predicts the cortical spread of Alzheimer's pathology. Nat Commun. 2016;7(1):13249.

- Grothe M, Heinsen H, Teipel SJ. Atrophy of the cholinergic basal forebrain over the adult age range and in early stages of Alzheimer's disease. Biol Psychiatry. 2012;71(9):805-813.
- Kilimann I, Grothe M, Heinsen H, et al. Subregional basal forebrain atrophy in Alzheimer's disease: a multicenter study. JAD. 2014;40(3):687-700.
- Budde MD, Janes L, God E, Turtzo LC, Frank JA. The contribution of gliosis to diffusion tensor anisotropy and tractography following traumatic brain injury: validation in the rat using Fourier analysis of stained tissue sections. *Brain*. 2011:134(pt 8):2248-2260.
- Vaillancourt DE, Spraker MB, Prodoehl J, et al. High-resolution diffusion tensor imaging in the substantia nigra of de novo Parkinson disease. Neurology. 2009;72(16):1378-1384.
- Boska MD, Hasan KM, Kibuule D, et al. Quantitative diffusion tensor imaging detects dopaminergic neuronal degeneration in a murine model of Parkinson's disease. Neurobiol Dis. 2007;26(3):590-596.
- Kerbler GM, Hamlin AS, Pannek K, et al. Diffusion-weighted magnetic resonance imaging detection of basal forebrain cholinergic degeneration in a mouse model. NeuroImage. 2013;66:133-141.
- Gómez-Isla T, Price JL, McKeel DW Jr, Morris JC, Growdon JH, Hyman BT. Profound loss of layer II entorhinal cortex neurons occurs in very mild Alzheimer's disease. J Neurosci. 1996;16(14):4491-4500.
- Laakso MP, Frisoni GB, Könönen M, et al. Hippocampus and entorhinal cortex in frontotemporal dementia and Alzheimer's disease: a morphometric MRI study. Biol Psychiatry. 2000;47(12):1056-1063.

- Devanand DP, Pradhaban G, Liu X, et al. Hippocampal and entorhinal atrophy in mild cognitive impairment: prediction of Alzheimer disease. Neurology. 2007;68(11): 828-836.
- Jack CR, Petersen RC, Xu YC, et al. Prediction of AD with MRI-based hippocampal volume in mild cognitive impairment. Neurology. 1999;52(7):1397-1403.
- Grothe M, Zaborszky L, Atienza M, et al. Reduction of basal forebrain cholinergic system parallels cognitive impairment in patients at high risk of developing Alzheimer's disease. Cereb Cortex. 2010;20(7):1685-1695.
- Li X, Jiao J, Shimizu S, Jibiki I, Watanabe K, Kubota T. Correlations between atrophy
 of the entorhinal cortex and cognitive function in patients with Alzheimer's disease
 and mild cognitive impairment: entorhinal cortex and cognitive function. Psychiatry
 Clin Neurosci. 2012;66(7):587-593.
- Gaetani L, Blennow K, Calabresi P, Di Filippo M, Parnetti L, Zetterberg H. Neurofilament light chain as a biomarker in neurological disorders. J Neurol Neurosurg Psychiatry. 2019;90(8):870-881.
- Mattsson N, Andreasson U, Zetterberg H, Blennow K; Alzheimer's Disease Neuroimaging Initiative. Association of plasma neurofilament light with neurodegeneration in patients with Alzheimer disease. JAMA Neurol. 2017;74(5):557.
- Rowe CC, Bourgeat P, Ellis KA, et al. Predicting Alzheimer disease with β-amyloid imaging: results from the Australian imaging, biomarkers, and lifestyle study of ageing. Ann Neurol. 2013;74(6):905-913.



Association of Cognitive Impairment With Free Water in the Nucleus Basalis of Meynert and Locus Coeruleus to Transentorhinal Cortex Tract

Winston Thomas Chu, Wei-en Wang, Laszlo Zaborszky, et al. Neurology 2022;98;e700-e710 Published Online before print December 14, 2021 DOI 10.1212/WNL.000000000013206

This information is current as of December 14, 2021

Updated Information & including high resolution figures, can be found at:

Services http://n.neurology.org/content/98/7/e700.full

References This article cites 50 articles, 7 of which you can access for free at:

http://n.neurology.org/content/98/7/e700.full#ref-list-1

Subspecialty Collections This article, along with others on similar topics, appears in the

following collection(s): **Alzheimer's disease**

http://n.neurology.org/cgi/collection/alzheimers disease

DŴI

http://n.neurology.org/cgi/collection/dwi
MCI (mild cognitive impairment)

http://n.neurology.org/cgi/collection/mci_mild_cognitive_impairment

MRI

http://n.neurology.org/cgi/collection/mri

Neuropsychological assessment

http://n.neurology.org/cgi/collection/neuropsychological_assessment

Permissions & Licensing Information about reproducing this article in parts (figures, tables) or in

its entirety can be found online at:

http://www.neurology.org/about/about the journal#permissions

Reprints Information about ordering reprints can be found online:

http://n.neurology.org/subscribers/advertise

Neurology ® is the official journal of the American Academy of Neurology. Published continuously since 1951, it is now a weekly with 48 issues per year. Copyright © 2021 American Academy of Neurology. All rights reserved. Print ISSN: 0028-3878. Online ISSN: 1526-632X.

